



**UNIVERSITÀ
DEGLI STUDI
DI PADOVA**



**DIPARTIMENTO
DI INGEGNERIA
DELL'INFORMAZIONE**

DIPARTIMENTO DI INGEGNERIA DELL'INFORMAZIONE

**CORSO DI LAUREA MAGISTRALE IN
BIOINGEGNERIA**

“Analysis of bursting phenomena in pancreatic beta cells”

Relatore: Prof. / Dott Morten Gram Pedersen

Laureando/a: Valerio Hoxha

Correlatore: Prof./Dott

ANNO ACCADEMICO 2022 – 2023

Data di laurea 17/04/2023

Contents

1	Abstract	6
2	Introduction	7
3	Biological background	9
3.1	Diabetes	9
3.1.1	Type 1 diabetes	9
3.1.2	Type 2 diabetes	9
3.2	Pancreas	11
3.2.1	Langerhans islets	12
3.3	Insulin	13
3.4	Gap junctions	15
3.5	Ion channels	16
3.5.1	Calcium dynamics	17
3.6	Hodgkin and Huxley model	18
3.6.1	Action potential dynamics	18
3.6.2	Nernst potential	19
3.6.3	Equivalent circuit	19
3.6.4	The model	21
4	Mathematical models	23
4.1	Single cell model	23
4.2	Couple of cells model	24
5	Model analysis and results	25
5.1	Slow-fast analysis	25
5.2	Single cell	26
5.3	Pair of identical cells	29
6	Discussion	31
6.1	Coupling between heterologous cells	31
6.2	Bifurcation surface	34
7	Conclusions	37
8	Bibliography	41

1 Abstract

This thesis is based on the works of Arthur Sherman and Gerda De Vries. Their simplified model for pancreatic β -cells was used under various circumstances. The primary objective of the thesis is to investigate, comprehend and explain the dynamics of the model under various circumstances. The analysis will go from the simplest case with two identical cells with the same initial conditions to the heterologous cells with diverse initial states. The secondary objective is to provide a geometrical perspective to the analysis, to help a better understanding of the system's dynamics.

2 Introduction

Pancreatic β -cells are a specialized type of cells located in the pancreas, organized in clusters called Islet of Langerhans. The cells are electrically coupled via gap junctions, and the oscillations are almost synchronous among the cells in an islet. When oscillating, these cells are able to secrete and produce the insulin hormone, which helps to regulate blood sugar levels. This happens thanks to the electrical activity that governs oscillations in the intracellular calcium concentration, which works as a trigger for the release of the hormone insulin. Insulin acts by stimulating the uptake of glucose by liver, muscles, and fat cells. It also inhibits the production of glucose by the liver, providing an essential tool that helps maintain healthy glucose levels in the body. When the glucose isn't in the physiological range, a pathological condition appears and is known as diabetes. There are two types of diabetes, type 1 that occurs when the immune system attacks and destroys the β -cells, resulting into inability to create insulin and consequently high level of glucose in the bloodstream emerge. Type 2 diabetes occurs when the pancreas isn't able to produce enough insulin or when the body becomes resistant to its effects, leading again to high levels of glucose. Glucose imbalances can lead into a range of health problems that can degenerate into blindness, kidney disease and vascular diseases.

From a mathematical standpoint, a simplified model for pancreatic β -cells has been used, with particular focus on the case of bursting. Bursting is a phenomenon that comes from a particular state of the system in which a fast subsystem and a slow subsystem interact, generating an alternation between an active phase with fast oscillations (called spikes) and a silent one. Bursting has an important physiological meaning, since it is the mechanism that is responsible for insulin secretion in response to blood glucose. In particular, the shape of bursting seen in β -cells is referred to as "square-wave" bursting, due to the wave form. Model dynamics have been examined through bifurcation analysis for various cases: single cell, coupled cells, coupled identical cells with different initial conditions, and coupling forces. The analysis has been performed using XppAUT and Matlab, in particular in XppAUT bifurcation diagrams were analyzed with the aim to explain the behavior of the model in the various cases through an analysis of the system dynamics. The main focus of the thesis was to better understand the behavior of the system under various circumstances, and to give a geometrical explanation of the model behavior. Parameters were chosen to expose key features of the system, not to achieve biophysical fidelity.

3 Biological background

In this section will be presented the biological background needed to give a context to the models and techniques used in this thesis. The description will start from the diabetes, going through the pancreas and its composition, ending with the dynamics of insulin secretion. An overview on the ionic channels and the junctions is needed too, since these are these mechanisms at the base for all the interactions that happen in the pancreas. A brief presentation of the Hodgking-Huxley work is done, since the beta cells model used in further sections is based on the one they invented.

3.1 Diabetes

Diabetes is a chronic disease characterized by elevated levels of blood glucose, and that occurs when the pancreas is not able to produce enough insulin or the body is not able to use the insulin it produces [1][2]. High level of glucose in the blood is a common effect of uncontrolled diabetes, and it may lead to serious damages to hearth, blood vessels, eyes, kidneys, and nerves over time. It has been estimated that more than 400 million people in the world live with diabetes [1]. There are two primary types of diabetes: type 1 and type 2, which are of significant interest to researchers, healthcare providers allover the world. Despite the similarities in the symptoms, the triggering causes of the two are very different.

3.1.1 Type 1 diabetes

The exact causes of this kind of diabetes are unknown, it's believed that the causes for type 1 diabetes are genetic and environmental, and currently it's not preventable. The majority of cases occur in children and adolescents. This disease is characterized by a lack of production of insulin from the body, so people with type 1 diabetes require controls and infusions of insulin daily. Without access to insulin, the patients could not survive. Symptoms include excessive urination and thirst, constant hunger, weight loss, vision changes and fatigue [1].

3.1.2 Type 2 diabetes

The causes for this kind of diabetes are related to an interlay between genetic and metabolic factors. Genetic factors combined to unhealthy lifestyles increase the risk. It was present only in adults, but recently it has begun to occur in children too. It is characterized by the inability of the body to use insulin. Type 2 diabetes accounts for the majority of diabetes cases in the world [2]. Symptoms are very similar to those of type 1 but often are less marked, making this kind of diabetes harder to detect, leading to complications [1].

Type 1 diabetes does not have specific risk factors, whereas type 2 diabetes has a multitude of them. Firstly, excessive body fat, lack of physical activity, and unhealthy diets are the strongest risk factors for type 2 diabetes. Overweight, obesity and physical inactivity are estimated to cause a large proportion of the global diabetes burden [3][1]. From recent studies, unhealthy diet habits are correlated to excessive body fat and type 2 diabetes risks. High intake of saturated fatty acids, high total fat intake, no consumption of fibers, high consumption of sugar sweetened beverages are all correlated with higher risks of type 2 diabetes. Active smoking is also a risk factor [4][1].

When diabetes is unchecked, complications could develop, contributing to rising in mortality, costs and poor quality of life. Over time, diabetes could damage the heart, blood vessels, kidneys, eyes, nerves, and increase the rate of heart failure and strokes. Diabetic retinopathy is an important cause of blindness and occurs when damage accumulates over time in the vessels of the retina. Recently, diabetes has been associated with increased rates of specific cancers and increased rates of physical and cognitive disabilities [5]. Diabetes is not only significant for the diseased, but it also has an important economic impact in the global health-care, this can be measured by direct medical costs, and indirect costs associated with productivity loss, and premature mortality [1]. The majority of risk factors of type 2 diabetes could be prevented by a behavioral change in the lifestyle of susceptible people. Improving diet and physical activity can prevent or delay the rising of type 2 diabetes on individuals at high risk. There are certain measures that can be implemented to encourage a healthy lifestyle, such as imposing taxes on unhealthy food and drinks and regulating their marketing. However, these actions often face resistance from industries that have vested interests in this area.

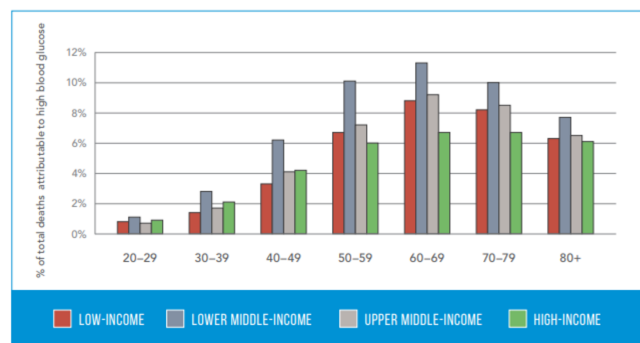


Figure 1: It can be observed that the problem is higher in the lower-middle income group. And as expected, it increases with age [1].

It has been estimated that in 2012 over 1.5 million death have occurred due to diabetes [1]. A lot of factors could be considered, in Figure 1 are presented the most common ones: deaths

attributed to high blood glucose by age and country income group. A further analysis of numbers and trends based on age and income has been made, but it goes beyond the purposes of this section, wanting to give a general knowledge of diabetes as a disease, its causes, its risk factors, and some possible solutions.

3.2 Pancreas

In a healthy adult, the pancreas weighs approximately 100g, has a length between 14 and 25 cm and is lobular and elongated in shape [6][7]. It is located behind the posterior and upper abdominal wall, it is divided in five anatomical parts: the head, uncinate process, neck, body and tail (Figure 2). It grows until the age of 30, varying in both weight and volume from individual to individual [6].

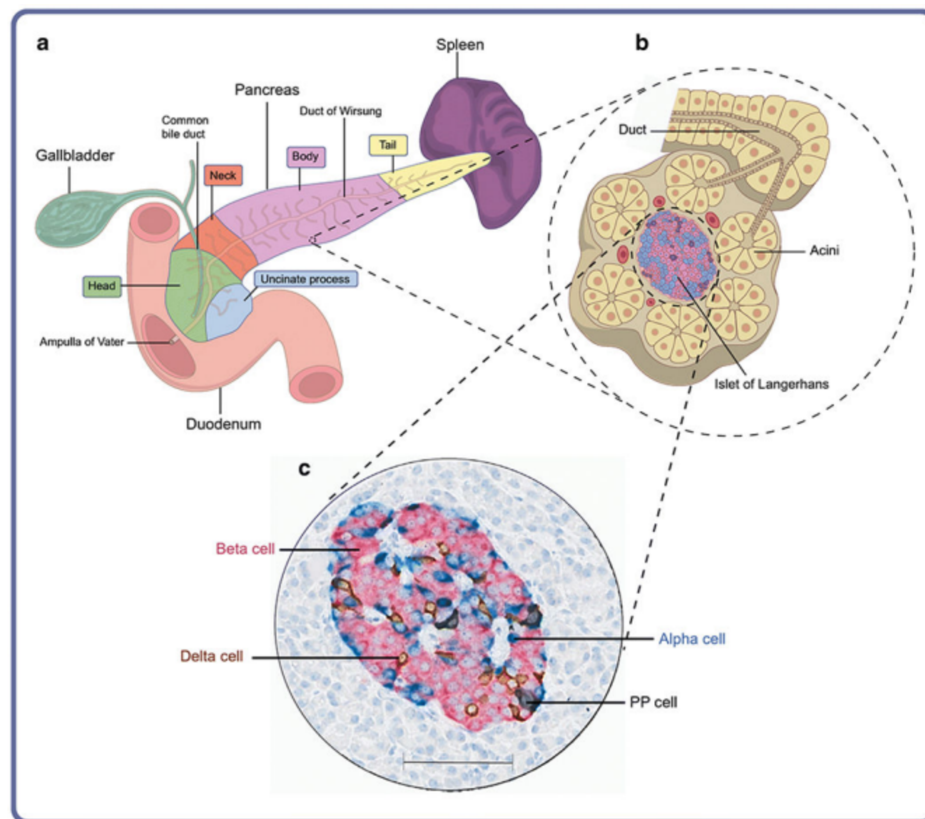


Figure 2: Key anatomical features of human pancreas. (a) Diagram of pancreas, and surrounding organs. (b) Schematic representation of organization of the endocrine and exocrine pancreas at the cellular level. (c) Human pancreatic islet showing the four endocrine cell types. Scale bar, $100\mu\text{m}$ [6].

The key component of the pancreas that will be analyzed in this thesis are the Langerhans islets, a cluster of specialized cells, responsible for secretion of hormones. In 1869, Paul

Langerhans made a significant discovery that marked a turning point in the history of diabetes research. This discovery alone initiated the research works in islet biology, insulin production, and glucose homeostasis, which has been a fertile field of research to this day.

3.2.1 Langerhans islets

The islets of Langerhans are an endocrine secretory tissue located between the clusters of acinar cells. It is estimated that there are around one million of these micro-organs. In humans, 40-60% of the endocrine cells are insulin producing β -cells, the rest are alpha, pancreatic polypeptide and epsilon cells which secrete glucagon, somatostatin, pancreatic polypeptide and ghrelin respectively. Each islet differs from the others in function of islet size, age and location in the organ. Smaller islets are composed mostly of beta cells, bigger islets may have equal numbers between alpha and beta cells, an example is presented in figure 3 [6]. Each islet is reached by one or more arteries that branch into capillaries, who emerges from the islet into small veins. Innervation is present too, motor nerve fibers carry impulses to both acinar cells and pancreatic islets. Parasympathetic fibers induce secretion of pancreatic juice as well they stimulate islets to secrete insulin, glucagon and other hormones required for blood glucose regulation. In contrast, sympathetic fibers cause inhibition of exocrine and endocrine secretions.

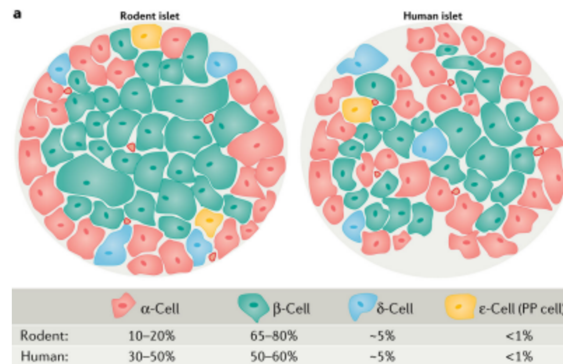


Figure 3: Comparison of the cellular composition of rodent and human islets. Rodent islets are made up of 10–20% of alpha cells, found predominantly on the outer mantle, and 65–80% of beta cells comprising their inner core. Delta cells, gamma cells (also known as or pancreatic polypeptide cells) and epsilon cells are found scattered throughout the islet. Human islets contain a higher percentage of alpha cells, which are found throughout the islet, and a slightly lower percentage of beta cells than rodents. [8]

The islets functions are regulated by signals initiated by autonomic nerves, circulating metabolites (glucose), circulating hormones and also by local hormones [6]. The role of pancreas in diabetic diseases is clear and simple to understand, since it secretes the two major hormones

that regulate the energy metabolism. Type 1 diabetes results from autoimmune mediated destruction of islet beta cells, this has been observed through autopsy performed on patients with the disease. The observations found out that 50-90% of islets had no beta cells, while having the other islet endocrine cells present with the expected number [6]. A reduced size of the pancreas has been observed in both individuals with type 1 and type 2 diabetes, being a predominant characteristic in the first case. The loss of the beta cells has been proposed as a mechanism for the size reduction, but it is not known if people with type 1 diabetes are born with a smaller pancreas, or it shrinks during the process [6]. Beta cells are capable of adapting to metabolic demand, trained athletes could secrete three times less insulin than untrained individuals, at the same time non-diabetic obese people can secrete up to five times more insulin in response to a glucose change. When the adaptation of beta cells fails, type 2 diabetes emerges [6]. Another factor that has been observed in the beta cells of individuals with type 2 diabetes is that the size is about 60% of normal beta cell mass. This, as in the case of shrinkage of the pancreas, is not known if it is a genetic predisposition so the people born with smaller beta cells are more likely to develop type 2 diabetes, or it depends on the lifestyle choices made by individuals.

3.3 Insulin

In the previous subsections, insulin has been discussed, here it will be described in more detail. Insulin is secreted by pancreatic beta cells in response to plasma level of glucose and additional signals like metabolic factors, neurotransmitters and hormone modulate insulin secretion [9]. "Glucose is the major factor controlling beta cell function and survival. Glucose entering the beta cell via glucose transporters is rapidly phosphorylated to glucose-6-phosphate by glucokinase and undergoes oxidation in mitochondria, leading to production of adenosine triphosphate (ATP). The rise of ATP/adenosine diphosphate ratio in the beta cell leads to subsequent closure of the KATP channel, which elicits cell membrane depolarization and allows the entry of Ca^{2+} through the opening of L-type voltage-dependent calcium channels. Raised levels of intracellular Ca^{2+} induce exocytosis of secretory granules containing insulin/proinsulin from pancreatic beta cell. The pharmacologic half-life of insulin is estimated to be between 5 and 8 minutes, and is mainly cleared by insulinase activity within the liver, kidneys, and some other tissues" [9]. Calcium is a key component in the insulin secretion mechanisms. The secretion of insulin occurs in two distinct phases: the first phase, a rapid early peak that peaks around 30 to 45 minutes after the meal, and the second phase, a slower and gradually rising peak that is also called basal insulin secretion, figure 4. Insulin's basic function, working together with glucagon, is to finely tune hepatic glucose production and modulate peripheral glucose utilization [10].

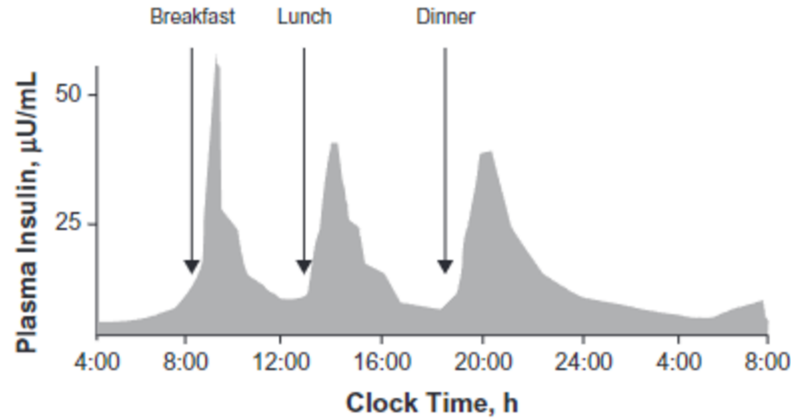


Figure 4: Physiologic insulin secretion during a day. [10]

From a chemical point of view, in the first phase, insulin secretion is stimulated by the increased cytosolic Ca^{2+} and is largely due to the exocytosis of primed insulin granules. Second phase insulin secretion is slow, activated by cytosolic Ca^{2+} , ATP, and cyclic adenosine monophosphate production, and due to the subsequent supply of new insulin granules for release. [9] In patients with type 2 diabetes, both aspects of insulin release can be markedly decreased or absent as the disease progresses. The role of insulin in the glucose homeostasis is represented by the direct effect of insulin on muscles and liver. These tissues require specific signaling pathways for insulin. In skeletal muscles, glucose utilization and storage is promoted by insulin that promotes glucose transport and net glycogen synthesis. In the liver, glycogen synthesis is activated, adipogenic gene expression is increased, and gluconeogenesis is inhibited by insulin. The impact of insulin may differ across different tissues, but the constituents involved in insulin signaling exhibit similarities among them. Furthermore, insulin suppresses glucagon secretion from pancreatic alpha cells, this phenomenon makes itself an inducer of hyperglycemia. [9] Utilizing insulin successfully, enhancing efficacy while reducing side effects, mimicking the physiologic profile of insulin secretion for both phases offers maximal effect [10]. Understanding the dynamics of insulin release and the mechanisms at its base could be crucial for improving tools for insulin intake in type 2 diabetic patients.

3.4 Gap junctions

Gap junctions are clusters of intercellular channels that allow direct diffusion of ions and small molecules between adjacent cells [11]. Connexons, comprising six connexin proteins that bind together, are responsible for creating the intercellular channels. The intercellular channels have different physiological properties, and they depend on the composition of the connexons. The connexons are located in the cellular membrane and when they dock together they form a gap between the cells which consents the communication between them (Figure 5). Communication occurs by biochemical signal exchanges through the intercellular channel.

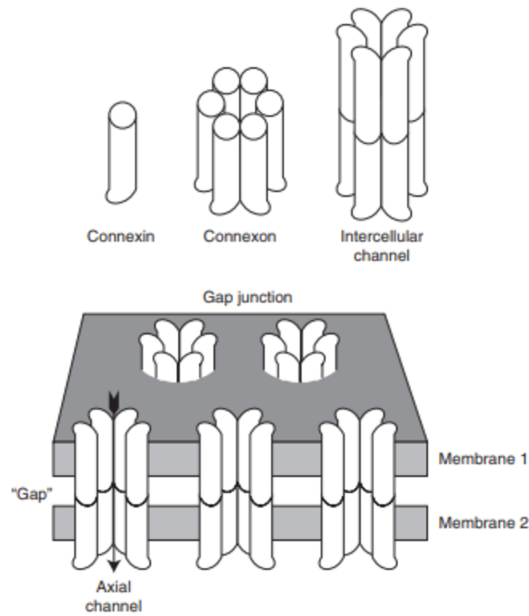


Figure 5: Gap junction structure is presented, connexin assembles into a connexon that is located in the membrane. When two connexons dock together from two adjacent cells, they assemble an axial channel forming the gap and consenting direct information exchanges.

Gap junctions consent the exchange of ions through a low resistance pathway. This is fundamental to the function of electrically excitable cells such as neurons, heart, smooth muscles, and also beta cells. Historically, gap junctions were discovered in the myocardium because of their properties of electrical transmission between adjacent cells. Gap junctions provide increased speed in synaptic transmissions and the ability to synchronize groups of cells for coordinated electrical and mechanical output, which is key for beta cells dynamics [11].

3.5 Ion channels

The cell membrane is a thin, flexible barrier that surrounds and separates the interior of a cell from its external environment. It is a semipermeable barrier made up of a phospholipid bilayer with embedded proteins and other molecules that perform various functions. Ion channels are specialized proteins that play a crucial role in the electrical signaling of living organisms. These channels allow the flow of specific ions such as sodium, potassium, calcium, and chloride across the cell membrane. They are essential for a wide range of physiological processes, including muscle contraction, hormone secretion, and neural communication. In recent years, there has been an increasing interest in the research field of ion channels, in part driven by the development of new techniques for studying these proteins at the molecular and cellular levels. These channels can be sorted into various groups based on ion type, ion selectivity, and gating. Voltage-gated ion channels are among the most studied and were modeled by Hodgkin and Huxley. Their groundbreaking work transformed our understanding of electrical signaling in neurons, and their findings were ultimately recognized with the award of a Nobel Prize. There are four different types of voltage-gated ion channels: potassium, sodium, calcium, and chloride [12].

Voltage-Gated Potassium Channels Voltage-gated potassium channels play a significant role in various physiological processes such as the repolarization of neural and cardiac action potentials, the regulation of Ca^{2+} signaling, control of cell volumes, as well as the facilitation of cellular proliferation and migration. These channels are formed by four separate polypeptide subunits, they are gated by neurotransmitters and membrane potentials, making them essential for excitatory inputs and electrical conduction. Action potentials changes in the membrane cause channel openings or closings, consenting a passive flow of potassium ions (K^+) from the cell to restore the membrane potential [12]. The potassium channel is depicted in green in Figure 6.

Voltage-Gated Sodium Channels Voltage-gated sodium channels play a significant role in initiation and propagation of action potentials in various cells including nerve, muscle, and other excitable ones. They are formed by a single large polypeptide chain containing four homologous domains. The channel consist of one α subunit and a smaller accessory β subunit [12]. The sodium channel is depicted in light blue in Figure 6.

Voltage-Gated Calcium Channels Calcium channels are vital for brain functionalities and in case of dysfunctions disorder as pain, epilepsy, ataxia, and migraine could emerge [13]. A calcium channel is depicted in yellow in Figure 6.

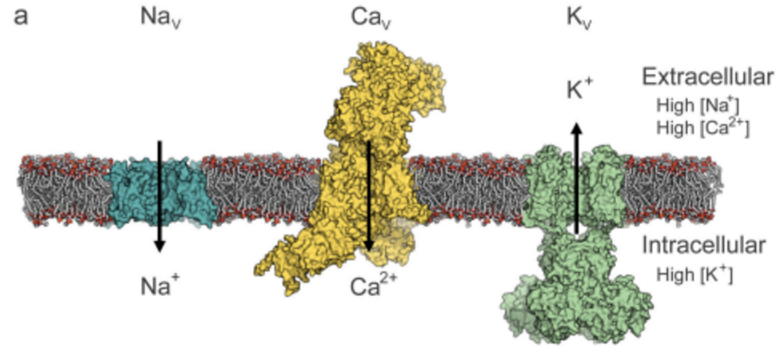


Figure 6: This is a model representation of sodium, calcium, and potassium channels across a membrane, where the arrows indicate the direction of ion flow [13].

3.5.1 Calcium dynamics

Bursting controls the influx of Ca^{2+} needed for insulin secretion [14], so a brief overview of calcium dynamics is needed. Concentration of Ca^{2+} in the cytoplasm is $>20,000$ times lower than outside the cell, this is achieved due to calcium transporting ATPases, sodium and potassium channels, and calcium binding proteins. When activated by an external stimulus, cells respond by increasing calcium in the form of spikes and oscillations, which subsequently regulate numerous cellular processes [15]. Cells contain numerous calcium binding proteins that act as sensors, or buffers, and sometimes as both. Calcium buffers are important since different buffers have different dynamics, leading to different calcium concentrations in the locations of the cell. Buffers make calcium dynamics finely tuned in both spatial and temporal extensions, making it a very precise signaling tool [15]. Overall, calcium buffering is a critical process for ensuring that cells maintain the appropriate levels of calcium ions, which is essential for their proper functioning. Research into calcium dynamics has advanced the comprehension of the stimulus-secretion coupling mechanisms in beta cells, and has also facilitated our comprehension of the pathogenesis of various diseases such as diabetes. Furthermore, this knowledge has the potential to enhance our understanding of drug administration, resulting in improved treatments.

3.6 Hodgkin and Huxley model

Hodgkin and Huxley (HH) were two British physiologists who made groundbreaking contributions to the understanding of the electrical properties of nerve cells and how they transmit information. In the 1940s and 1950s, they conducted a series of experiments on giant axons of squids using the voltage clamp technique, and discovered that the electrical signals in nerve cells were caused by the flow of ions across the cell membrane. Afterward, they developed a mathematical model to explain this phenomenon, which became known as the Hodgkin-Huxley model. Their model accurately describes the behavior of voltage-gated ion channels, and it is still influential and relevant in the fields of neuroscience and biophysics.

3.6.1 Action potential dynamics

The cell membrane of neurons is a voltage-gated ion channel, which has high selectivity for ions present inside the cell and outside it. The transmembrane current depends on the rapid inward current caused by sodium and the slow outward current caused by potassium [16]. Sodium channels are the first to open, letting the ions flow inside the cell, depolarization begins, and the action potential is generated. After that, sodium channels close and potassium channels are opened, letting ions escape from the cell, repolarization is achieved. In the end, the membrane undergoes a hyperpolarization phase, in which the membrane potential goes back to a resting state, Figure 7.

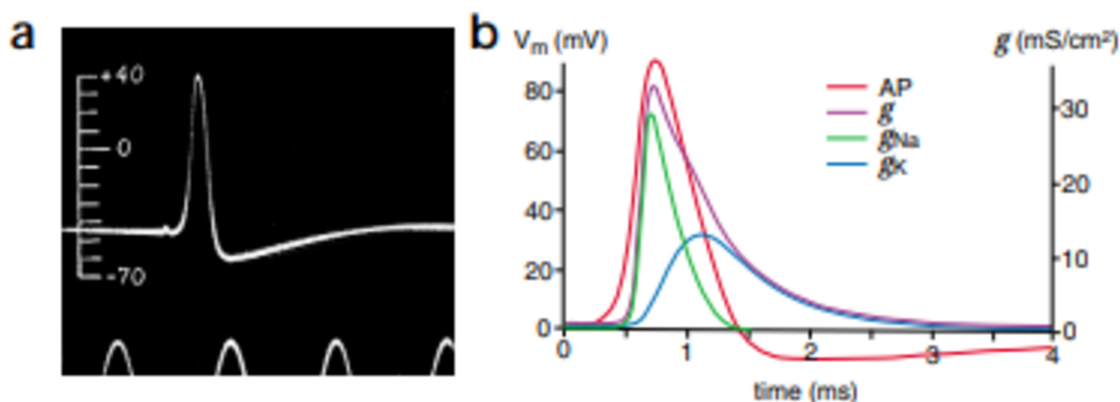


Figure 7: a) First recording of an action potential, from squid axon. b) Ionic conductances separated, with the actual action potential as reference [17].

3.6.2 Nernst potential

The Nernst potential, is the equilibrium potential for a single ion across a cell membrane. When an ion is at equilibrium across a membrane, the concentration gradient and electrical gradient are balanced, resulting in no flow of ions across the membrane. The Nernst potential is the voltage at which this equilibrium is achieved for a particular ion. The Nernst potential has an important role for the HH model, as it provides an instrument useful for calculating the driving force of each ion that contributes to membrane potential. The driving force is calculated as the difference between the Nernst potential of a single ion and the actual membrane potential. From there, the net flow of ions through the membrane could be calculated.

$$V_{Nernst} = \frac{61.5}{z} \log_{10} \frac{[ion]_{out}}{[ion]_{in}}$$

So, summing up, the Nernst potential represents the resting potential for each ion, and is 61 mV for sodium and -90 mV for potassium.

3.6.3 Equivalent circuit

Cell membrane could be modeled with an equivalent circuit, which is a simplified electrical circuit that represent the behavior of the membrane in response to electrical stimuli. The model includes:

1. Capacitance: This represents the cell membrane, since it acts as a capacitor storing charges across its surfaces.
2. Resistance: This represents the lipid bilayer, since it acts as a resistor to the flow of electrical current. The ion channels also conduct currents with a resistance R.
3. Ionic batteries: They create voltage difference across the membrane $V = V_{in} - V_{out}$.

This circuit could be resolved easily using the Kirchoff's law:

$$0 = I_{Cap} + I_{Na} + I_K + I_{leak} - I_{app}$$

That replacing them with the formulas of the capacitive current and the Ohm's law, the sequent equation is obtained:

$$C_m \frac{dV}{dt} = -g_{Na}(V - V_{Na}) - g_k(V - V_K) - g_L(V - V_L) + I_{app}$$

Where V_{Na} and V_K are the Nernst potentials for each ion. An example of circuit is shown in Figure 8.

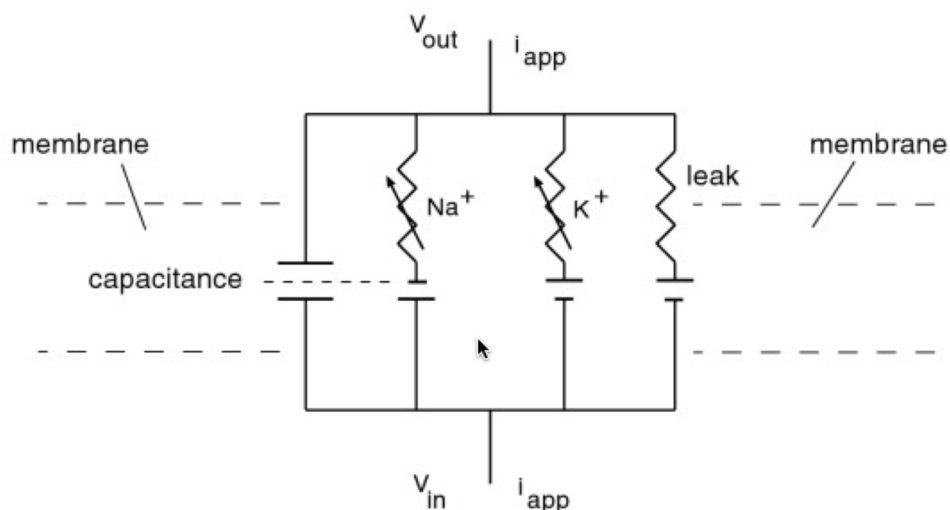


Figure 8: Equivalent circuit, capacitance is present, also the ion pumps for sodium and potassium. A leak current is taken in account since the membrane isn't a perfect isolator.

This system does not simply approach the equilibrium, because the conductance depends on the dynamics of V . To find the dynamics of V , HH opened the feedback loop and used the Voltage clamp technique.

Voltage clamp The voltage clamp technique involves applying a controlled voltage across the cell membrane while simultaneously measuring the resulting current flow. By maintaining a constant voltage across the membrane, the technique allows researchers to measure the ionic currents flowing through specific channels or transporters in the membrane. The injected current is kept equal to I_{mem} , so it can be measured. By using this method, HH successfully determined the behavior of sodium and potassium and formulated a mathematical equation that accurately portrays the channels' dynamics and characteristics throughout time.

3.6.4 The model

Thanks to the voltage clamp technique, the potassium conductance, the sodium conductance and the leak current are described as:

$$\begin{aligned} g_K &= g_{Kmax}n^4 \\ g_{Na} &= g_{Namax}m^3h \\ g_L &= g_{Lmax} \end{aligned}$$

$g_{Kmax}, g_{Namax},$ and g_{Lmax} denote the maximum values of potassium, sodium, and leak conductances and are parameters equal to 36, 120, and 0.3 $\text{Ohm}^{-1}\text{cm}^{-2}$ respectively [16]. In these formulas are present $m, n,$ and h that express the gate controlled variables of ion channels, they have their own dynamics:

$$\begin{aligned} \frac{dm}{dt} &= \frac{m_\infty(V) - m(V)}{\tau_m} \\ \frac{dn}{dt} &= \frac{n_\infty(V) - n(V)}{\tau_n} \\ \frac{dh}{dt} &= \frac{h_\infty(V) - h(V)}{\tau_h} \end{aligned}$$

The time constants τ_x change with $m, n,$ and $h,$ accordingly. α is the transition rate that characterizes the ion channels that change from closed to open, β the channels that go from open to closed. $m_\infty, n_\infty,$ and $h_\infty,$ are the steady state values of the gate variables $m, n,$ and $h,$ accordingly. They are all functions of membrane potential [16].

$$\begin{aligned} x_\infty &= \alpha_x / (\alpha_x + \beta_x), \quad x = m, n, h \\ \tau_x &= 1 / (\alpha_x + \beta_x), \quad x = m, n, h \end{aligned}$$

Now that every part has been explained, the full HH working model is summarized by:

$$\begin{aligned} I_{Cap} &= I_{Na} + I_K + I_{leak} + I_{app} \\ C_m \frac{dV}{dt} &= -g_{Na}m^3h(V - V_{Na}) - g_Kn^4(V - V_K) - g_L(V - V_L) + I_{app} \\ \frac{dm}{dt} &= \frac{m_\infty(V) - m(V)}{\tau_m} \\ \frac{dn}{dt} &= \frac{n_\infty(V) - n(V)}{\tau_n} \\ \frac{dh}{dt} &= \frac{h_\infty(V) - h(V)}{\tau_h} \end{aligned}$$

4 Mathematical models

The mathematical model used is based on a simplified version of a biophysically based model for bursting in pancreatic β -cells [19][20], tuned for the various cases studied. The models were computed in XPPAUT, the bifurcation diagrams were obtained in AUTO and imported in Matlab for aesthetic purposes.

4.1 Single cell model

The initial scenario examined involves a mathematical model with a single cell, it is the simplest case study and acts as a base for the models with multiple cells. The single cell is able to burst under certain conditions and parameters. The model equations are (1)-(3), below are presented some support equations, all with their own biological meaning. The parameters are selected to emphasize the critical characteristics of the system, rather than to achieve biophysical accuracy.

$$\tau \frac{dV}{dt} = -I_{Ca}(V) - I_k(V, n) - g_s S(V - V_k) \quad (1)$$

$$\tau \frac{dn}{dt} = \lambda(n_\infty(V) - n) \quad (2)$$

$$\tau_S \frac{dS}{dt} = S_\infty(V) - S + \beta \quad (3)$$

The model uses these support equations:

$$I_{Ca}(V) = g_{Ca} m_\infty(V)(V - V_{Ca})$$

$$I_K(V) = g_K n(V - V_K)$$

$$x_\infty(V) = \frac{1}{1 + \exp((V_x - V)/\Theta_x)} \quad x = m, n, S$$

Parameters are presented in Table 1.

$g_{Ca}=3.6$	$V_{Ca}=25$ mV	$V_m=-20$ mV	$\theta_m=12$ mV	$\tau=20$ msec
$g_K=10$	$V_K=-75$ mV	$V_n=-16$ mV	$\theta_n=5.6$ mV	$\tau_S=35$ msec
$g_S=4$		$V_S=-45$ mV	$\theta_S=10$ mV	$\lambda=0.8$

Table 1

Equation (1) refers to the current balance equation discovered by Hodgkin-Huxley. V represents the membrane potential, and t the time. The model includes all the features needed for

a biophysical model of square-wave bursting: a fast inward current (I_{Ca}), a slower outward current (I_k) and a slow variable (S) that switches the active spiking phase with the silent one. I_{Ca} and I_K represents the voltage-activated calcium and potassium currents, the calcium current is assumed to respond instantaneously to a change in membrane potential while the potassium dynamics are governed by the gating variable n via equation (2). These two currents are responsible for generating action potentials during the active phase of bursting. S is an abstraction of a mechanism in which an inhibitory K^+ current is present due to Ca^{2+} or ADP. Notably, the I_k is governed by the dynamics of the activation variable n via equation (2). Since $\tau \ll \tau_S$ we can decompose the system into a fast subsystem composed by the (1) and (2) equations and a slow subsystem with the (3) equation, from there a slow-fast analysis could be performed, using S as a bifurcation parameter. To enable cell heterogeneity the β parameter is added, and it will be changed to achieve it. This model summarizes the behavior of a single cell, the most interesting cases use at least two coupled cells using the same equations for every cell. The equations and the parameters will be indexed with i for the first cell and j for the second one.

4.2 Couple of cells model

To simulate the behavior of 2 cells coupled, only a coupling resistance (g_c) is needed and the variables V , n and S are indexed by cell number (i, j). The coupling term (g_c) is added to the V equation as shown in equation (4). Altering this parameter has an important role in the dynamics between the two cells [20].

$$\tau \frac{dV_i}{dt} = -I_{Ca}(V_i) - I_k(V_i, n_i) - g_S S_i (V_i - V_k - g_c (V_i - V_j)), i, j = 1, 2 \quad (4)$$

β -cells are connected by gap junctions, so it makes sense that there is not coupling on the auxiliary variables n or S . Note that β is also indexed with i - j as for the cells, in this work the β_i is never changed, and instead the parameter β_j is the one that will be modified, usually.

5 Model analysis and results

As already said, the analysis were performed using xppAUT, the graphs were then imported into Matlab for aesthetic purposes. The method employed is commonly referred to as slow-fast analysis.

5.1 Slow-fast analysis

Components that interact in different timescales is a frequently occurring situation in biological systems. For example, there is a huge gap in timelines between neuronal electrical activity and circadian rhythms coordinated through the suprachiasmatic nucleus of the hypothalamus and involving rhythms in gene expression [18]. These examples are especially problematic for computer simulations of mathematical models, because they are very expensive from a computational point of view. A system that evolves i two timescales could be written as:

$$\begin{aligned}\frac{dx}{dt} &= F(x, y) \\ \frac{dy}{dt} &= \epsilon G(x, y)\end{aligned}$$

where $\epsilon > 0$ is very small. In this model, x evolves faster than y. We can refer to the x equation as the fast subsystem, while the y will be the slow subsystem [18].

The general approach of fast-slow analysis is to treat the two subsystems separately. The idea is that for general initial conditions, the system will be governed by fast subsystems, and it will settle to a fast subsystem attractor, where $F=0$, that is parameterized by y. In this neighborhood, the system will follow the slow subsystem, until a boundary of the attractor is reached, and the fast subsystem takes over again.

John Rinzel adapted the fast-slow analysis technique to understand the dynamics underlying bursting in neurons and pancreatic beta cells. It has been shown that it is more effective in evoking neurotransmitter and hormone secretion than continuous trains of action potentials. Fast-slow analysis is now regularly used in analysis of bursting oscillations [18], and is the technique used in this thesis for obtaining and commenting results.

5.2 Single cell

The first analysis was performed with the model for a single cell. The initial conditions were $v=-65$, $n=0$, $s=0.15$.

To obtain the bifurcation diagrams the model is plotted using (5), there is a parameter called *autoc* which changes between 0 and 1, so it allows switching between the original model or one where the dynamics of s are simplified.

$$ds/dt = autoc * (cknot - s) + (1 - autoc) * (sinf - s + betaj)/taus \quad (5)$$

This trick allows plotting the bifurcation diagrams in xppAUT. The parameter *cknot* is used to simplify the model, in particular is the parameter used by AUTO to obtain the bifurcation diagrams. The bifurcation diagram obtained is presented in Figure 9.

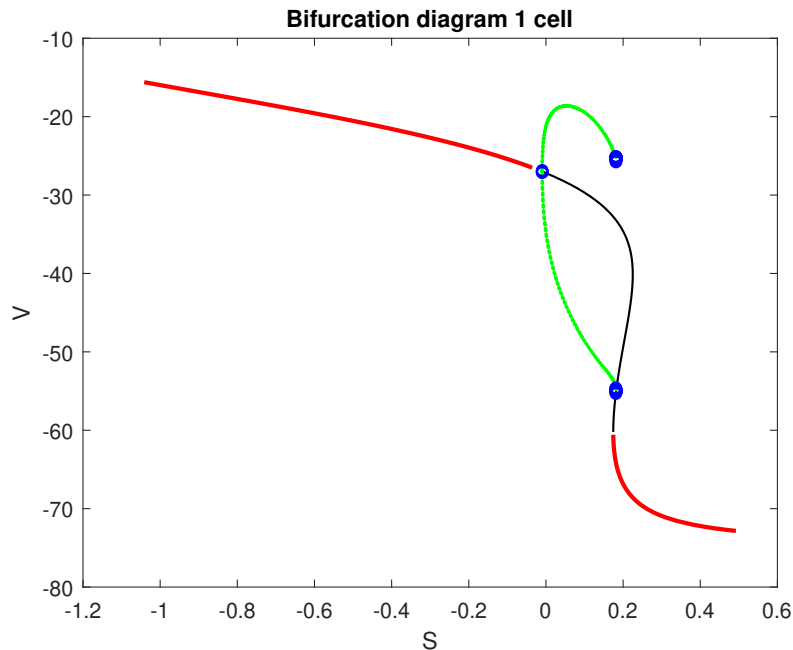


Figure 9: The red branch represents the stable points, the black one represents the unstable ones. The green C shaped curve represents the limit cycles. The blue circle represents the Hopf Bifurcation.

As already said, since the time scales of s are much slower than the one of V and n , S can be used as a bifurcation parameter. The red branches are the steady state solutions, those branches attract the dynamic of the system into a stable solution. The black branch represents the unstable solutions, and there we have the saddle points from which the model tends to escape. In green are represented the maximum and minimums of the Limit Cycles,

there the model oscillates until is able to "escape" from there. These dynamics of attraction and repulsion could be seen easily from Figure 10.

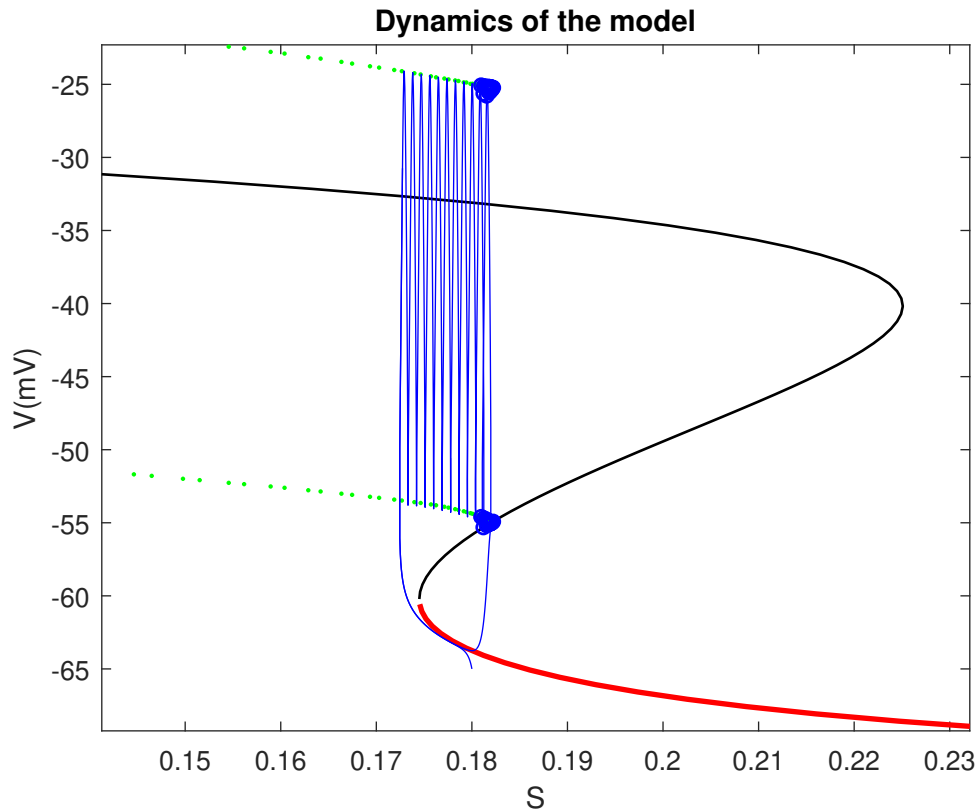


Figure 10: This graph represents one bursting cycle. The blue line is the model evolution over time, the model follows/escapes from the bifurcation diagram as expected and jumps from Max to min of the Limit Cycles.

For the steady solutions the system stabilizes himself to a fixed point, for the unstable solutions the cell starts to spike continuously. This shows that one cell alone is capable of spiking or being silent using the proper parameters, figure 9.

A Hopf bifurcation (HB) is present for $cknot = -0.009744$ (blue circle in figure (9)), from there the limits cycle (LC) emerge. In figure 9, the C shaped curve represents the branch of limit cycles. The upper part represents the maximums of V during the oscillations, the lower part represents the minimums. During bursting, the spikes are contained between those two branches until the dynamics are able to escape to the stable solutions, it can be observed from figure 10. For $cknot = 0.1745$ a saddle-node bifurcation is present. The key for understanding bursting is represented by the bistability that the model could achieve between the low voltage steady state represented by the lower red curve and the silent phase of bursting and the stable limit cycle oscillations, representing the active phase of bursting,

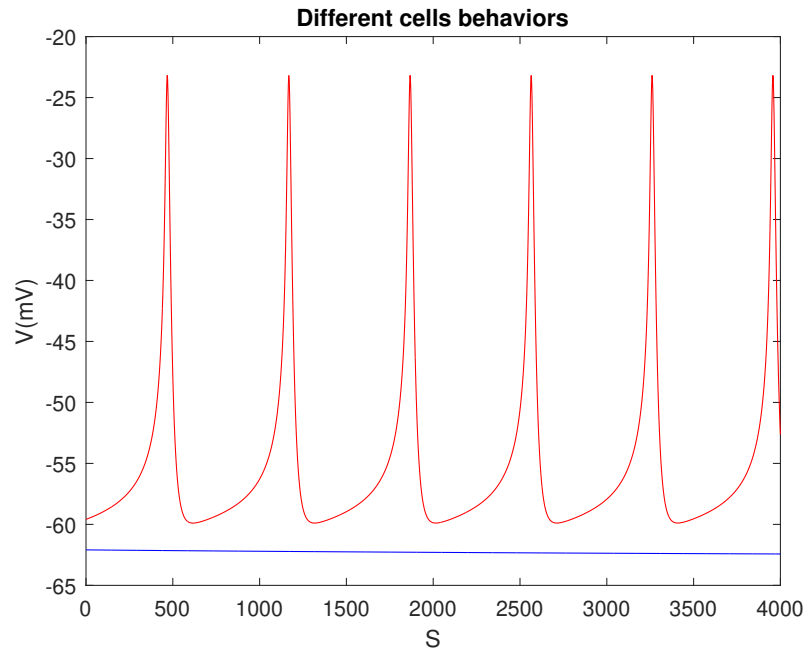


Figure 11: The red line represents the cell spiking. The blue line represents the cell resting. Those dynamics were obtained changing lambda to 0.8 for both cases and using $\text{betaj}=0$ for the red dynamic, and $\text{betaj}=0.1$ for the blue dynamic.

this is depicted in figure 10.

5.3 Pair of identical cells

The analysis for a pair of identical cells is performed using the model with formula (4) providing the coupling parameter g_c and without changing the β parameters for the two cells. For $g_c=0$ the figure 12 was obtained, showing that the two cells are not in the same state for the parameter selected. Changing this parameter leads to different dynamics between the two cells.

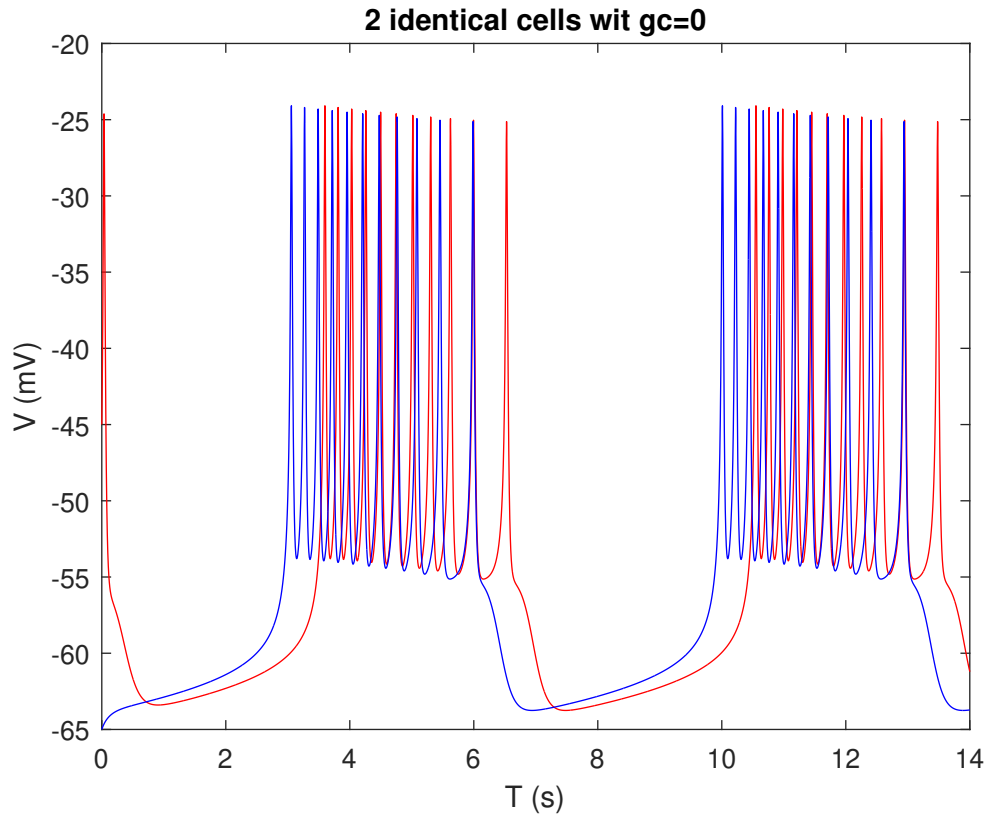


Figure 12: The blue line represents the i-cell, the red line represents the j-cell. In this case, $g_c=0$.

The initial parameters are chosen identical apart from V , $V_i = -34$, and $V_j = -45$, this was done because with identical cells the graphics would be overlaying and would be hard to distinguish the cells, in this way only a shift in the timescale is expected to happen. Without coupling, the dynamics of the cells are disconnected one from the other, but they have the same pattern, as expected from the initial conditions difference they are identical but shifted in time, this can be observed easily from the figure 12.

Introducing a coupling between the cells, a different behavior could be observed. For $g_c=0.04$ the two cells have the same period, but the bursting spikes are in antiphase. The initial

conditions are identical to the ones for $g_c=0$.

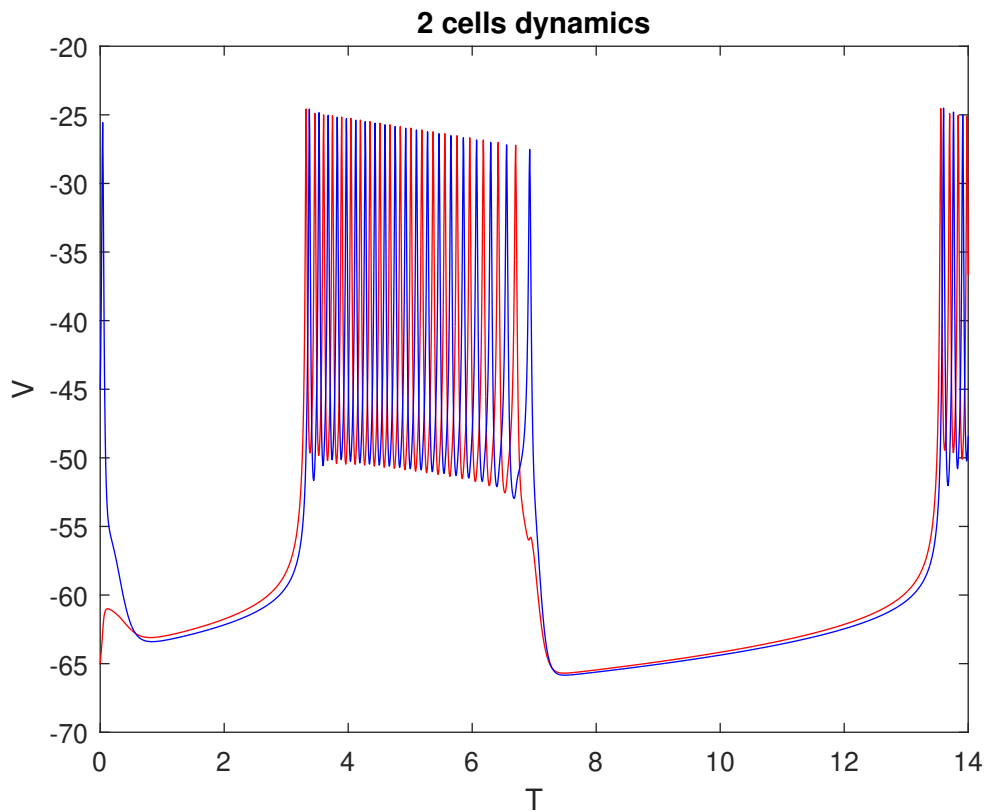


Figure 13: The blue line represents the i-cell, the red line represents the j-cell. In this case, $g_c=0.04$.

In this scenario the two cells synchronize in period, to a further look an antiphase between the spikes could be noted. For other values of g_c the behavior of the model with identical cells is similar to the one obtained in figure 13, so for practical reasons further graphs are not shown.

6 Discussion

Now that the simplest cases have been analyzed and described, in this section cases with heterogeneity will be explored and discussed, trying to understand and explain the behavior of 2 different cells in totally different initial situations are coupled by different coupling strengths.

6.1 Coupling between heterologous cells

β_j was set to 0.1 to simulate two different cells. The first case analyzed was with $g_c=0$, the j-cell doesn't present any bursting, it stays in a resting state as shown in figure 14, as expected from what seen with the single cell behavior. So, with the absence of coupling, the two cells are disconnected one from the other, and their dynamics remain unaffected by each other.

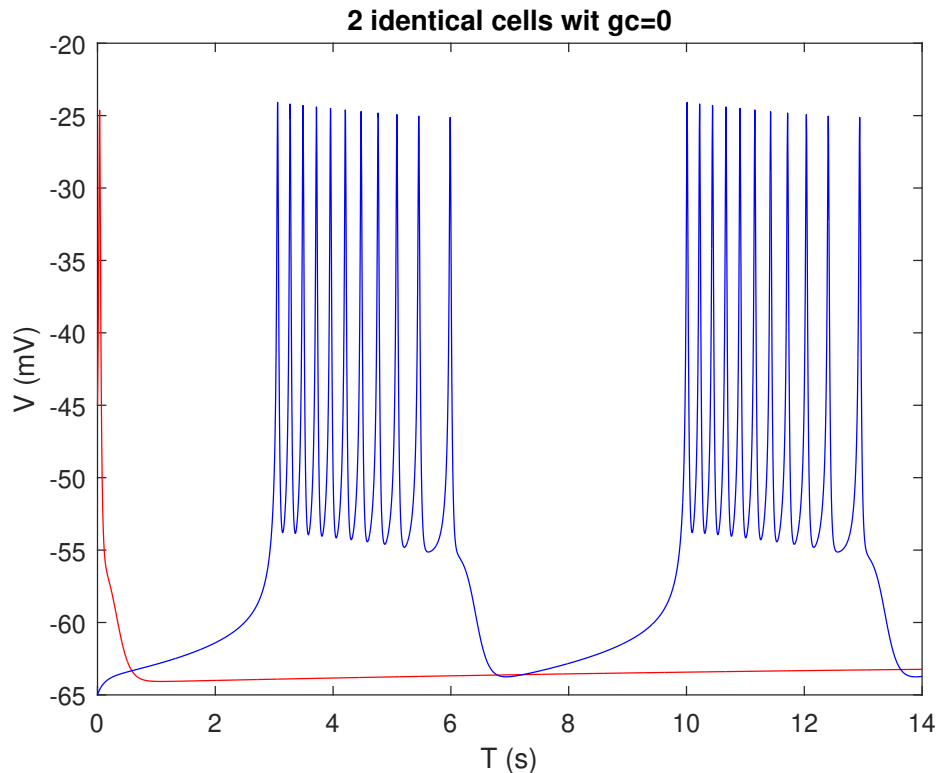


Figure 14: The blue line represents the i-cell, the red line represents the j-cell. With the introduction of β_j , the j-cell is not able to spike and is in a state of rest as seen for the single cell.

The cells are identical, in every parameter apart for β_j , which makes the red cell unable to burst by herself.

With $g_c=0.04$ a more interesting behavior appears. The j-cell isn't quiescent anymore, some new kind of bursting patterns appear, depicted in figure 15. The j-cell undergoes a state in

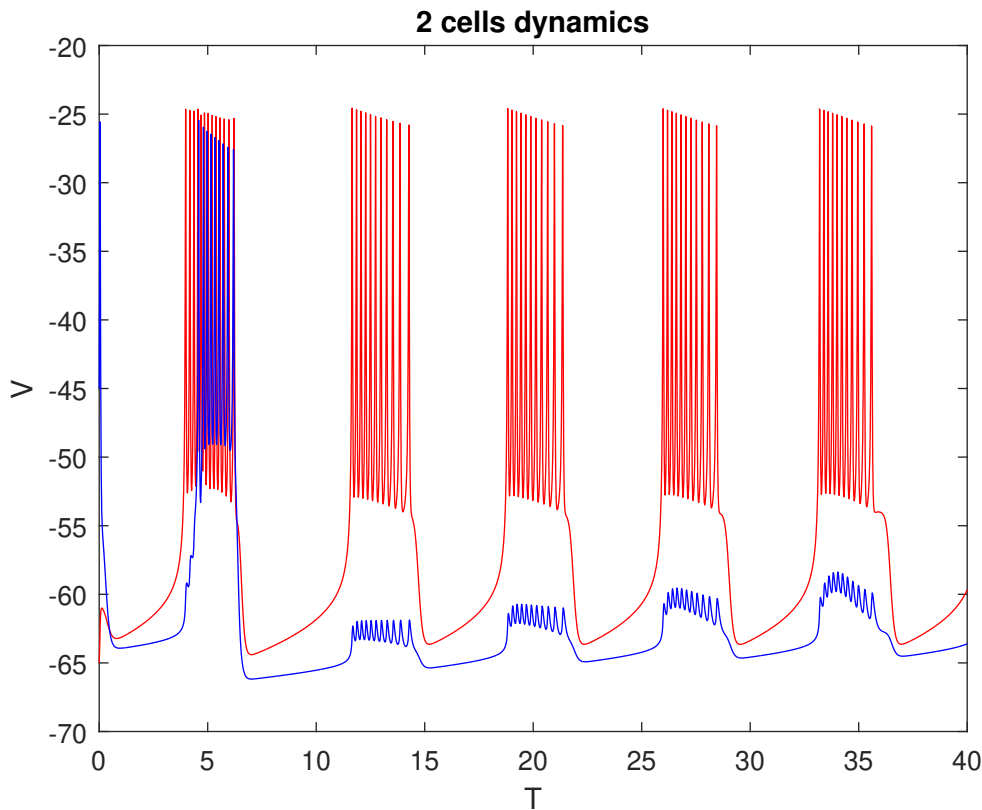


Figure 15: The blue line represents the i-cell, the red line represents the j-cell. It can be easily seen that the j-cell bursts follow the i-cell in period, but it isn't able to burst as it used when the cells were identical. Amplitude raises after every burst until it reaches a point in which it burst as the i-cell, then after that it goes down and starts rising again.

which the burstings are very different over time. It starts with a smaller burst than the i-cell in both amplitude and period. The burst increases with time until it becomes similar to the burst observed for the single cell. After the big burst appears, the systems restarts all over into a pattern that is pseudo-periodic. To explain this particular behavior, a particular type of analysis is performed. Bifurcation diagrams are calculated for the 1 cell model with g_c for fixed values of V_j . The diagrams obtained are different for different values of V_j , they appear to shift, and the knees become more gentle as V_j grows. The diagrams were imported in Matlab to obtain the figure 16, for V-S plane, in which can be observed that the random oscillations are contained between the two bifurcation diagrams for $V_j=-44$ and $V_j=-63$.

The dynamic is very interesting since the cell oscillates between two states of stability in accord to what happens to the i-cell. It is able to fully burst when the system surpasses the

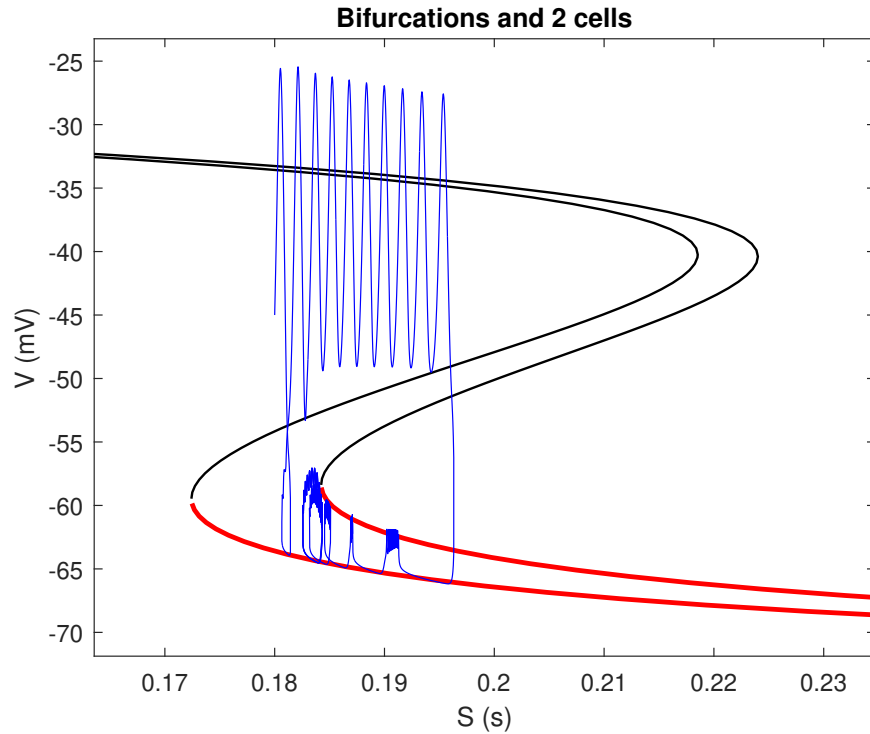


Figure 16: The blue line is the dynamic of the j-cell. The lower bifurcation diagram refers to the 1 cell model with $V_j=-44$, the upper refers to $V_j=-63$.

stable points of the upper bifurcation diagram. It can be imagined as the upper bifurcation diagram is attracting the model every time a small oscillation is present, then when the upper branch is not stable anymore the system fires a proper burst, finding himself trapped in the limit cycles until it eventually escapes from there as in the case for single cells, returning trapped between the two stable branches depending on the state of the i-cell. Similar analysis were performed for other values of g_c . The results for lower g_c were not appreciable, while for higher ones the small burst tend to get bigger, making it harder to recognize the pattern, so were not reported as they were considered less interesting or redundant. The interesting range is present for $g_c=0.03-0.1$. A new idea to better explain this behavior emerges, the dynamics of the model should move into a "bifurcation surface", obtained by an interpolation of bifurcation surfaces calculated varying V_j .

6.2 Bifurcation surface

To obtain the bifurcation surface, an interpolation of the bifurcation diagrams is needed, and it is obtained by plotting the bifurcation diagrams for V_j in the range -26-64 mV. Limit cycles are also depicted in the figure 17 to help the comprehension of the model from comparisons between 2D and 3D diagrams. In this case has been used a $gc=0.05$.

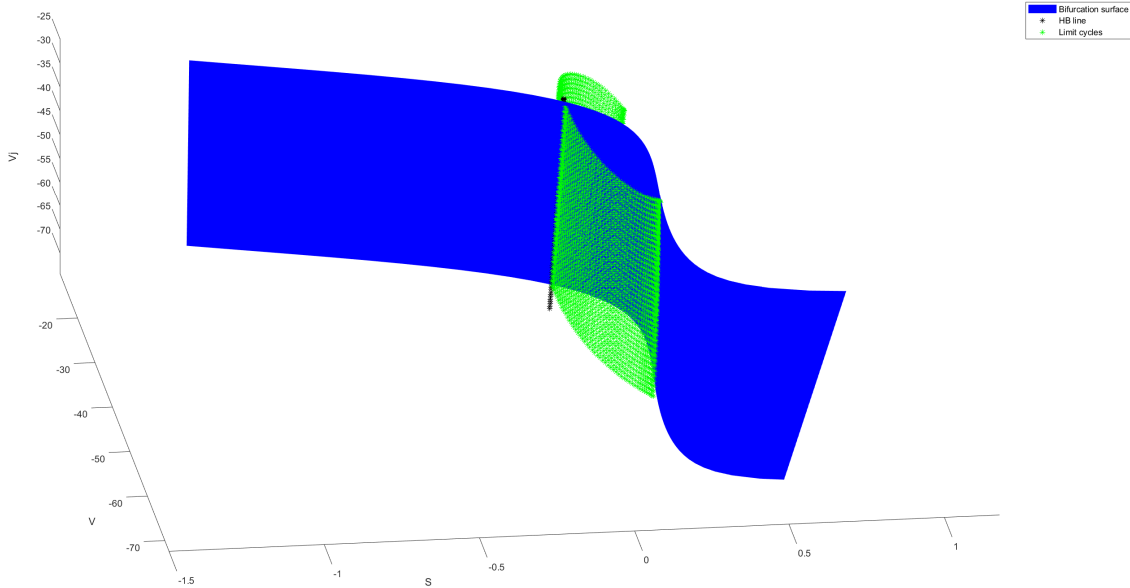


Figure 17: In blue is presented the bifurcation surface. The black stars represent the Hopf Bifurcation points. In green stars are presented the Limit Cycles.

After obtaining the bifurcation surface, the dynamics of the model were added in red, it can be observed that it travels near the surface, going from small spikes to the bigger ones, as depicted in both graphics in figure 18. It can be observed that the model displays big burst oscillations for higher values of V , and those bigger oscillations follow the limit cycles until eventually the model is able to escape from there. Another interesting observation is that while bursting in the V - S plane, the dynamic of V_j is present, causing the model to "surf" the bifurcation surface. In particular, this is observed for values of S around 0.207. Going further, after the big burst the model shoots down the dynamics line and reaches the bifurcation surface, that is known to present stable solutions for low values of V and high values of s (from the 2D analysis).

At this point, the model starts to go slowly backwards in the S scale, following the stable solutions. Here it can be observed that the small burst began to fire in the V - S plan, this can

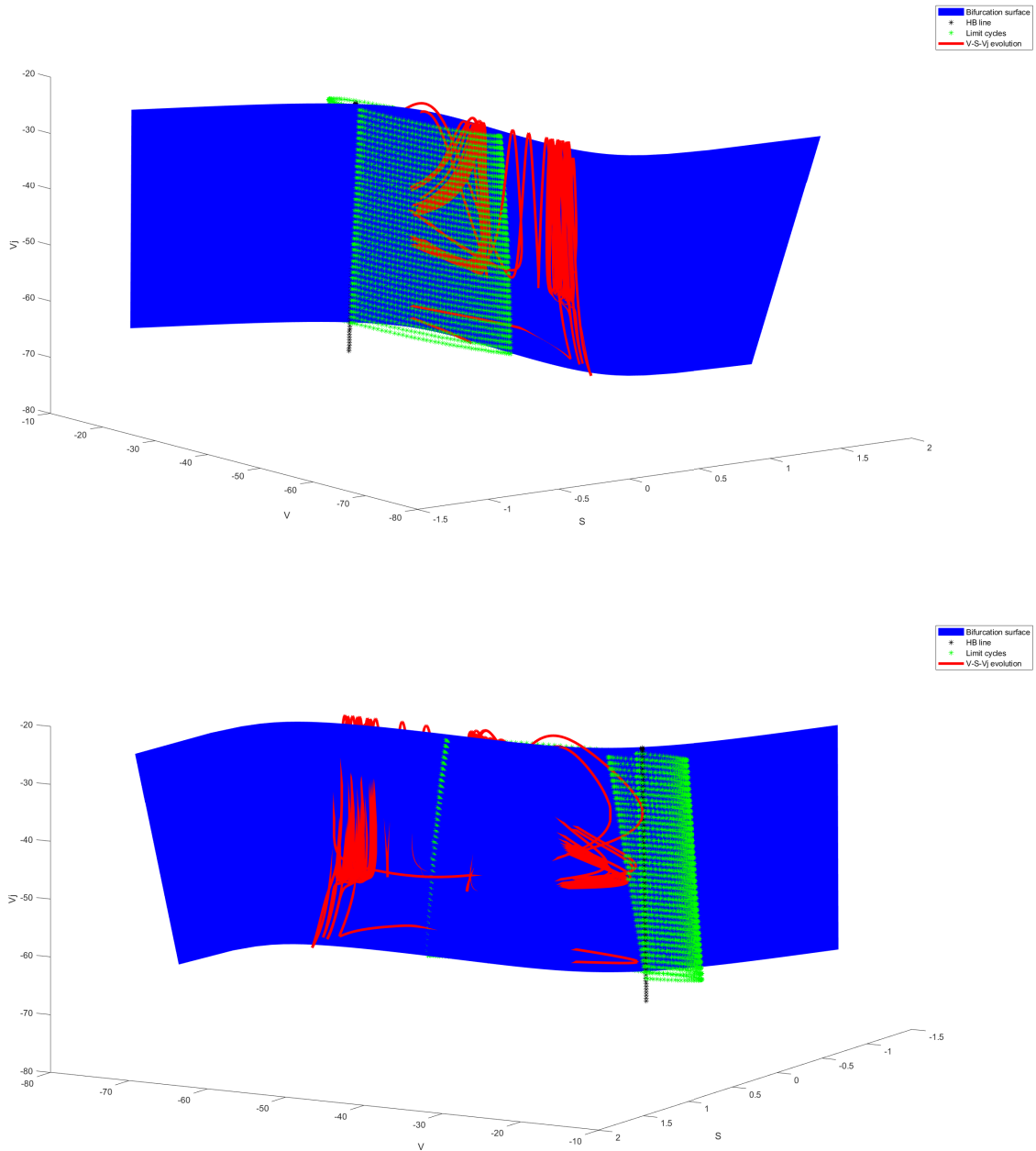


Figure 18: Blue, green and black points have the same meaning as in the 17 figure. In red is presented the evolution of the cells dynamics. Two points of view are presented so the dynamic could be observed under and over the surface.

easily be explained looking at the 3D graphic. The dynamics of V_j takes over, and horizontal oscillations are visible in the surface, it can be observed in the V - V_j plane. Bursts get bigger and bigger over time, following the curvature of the surface. At some point the model goes

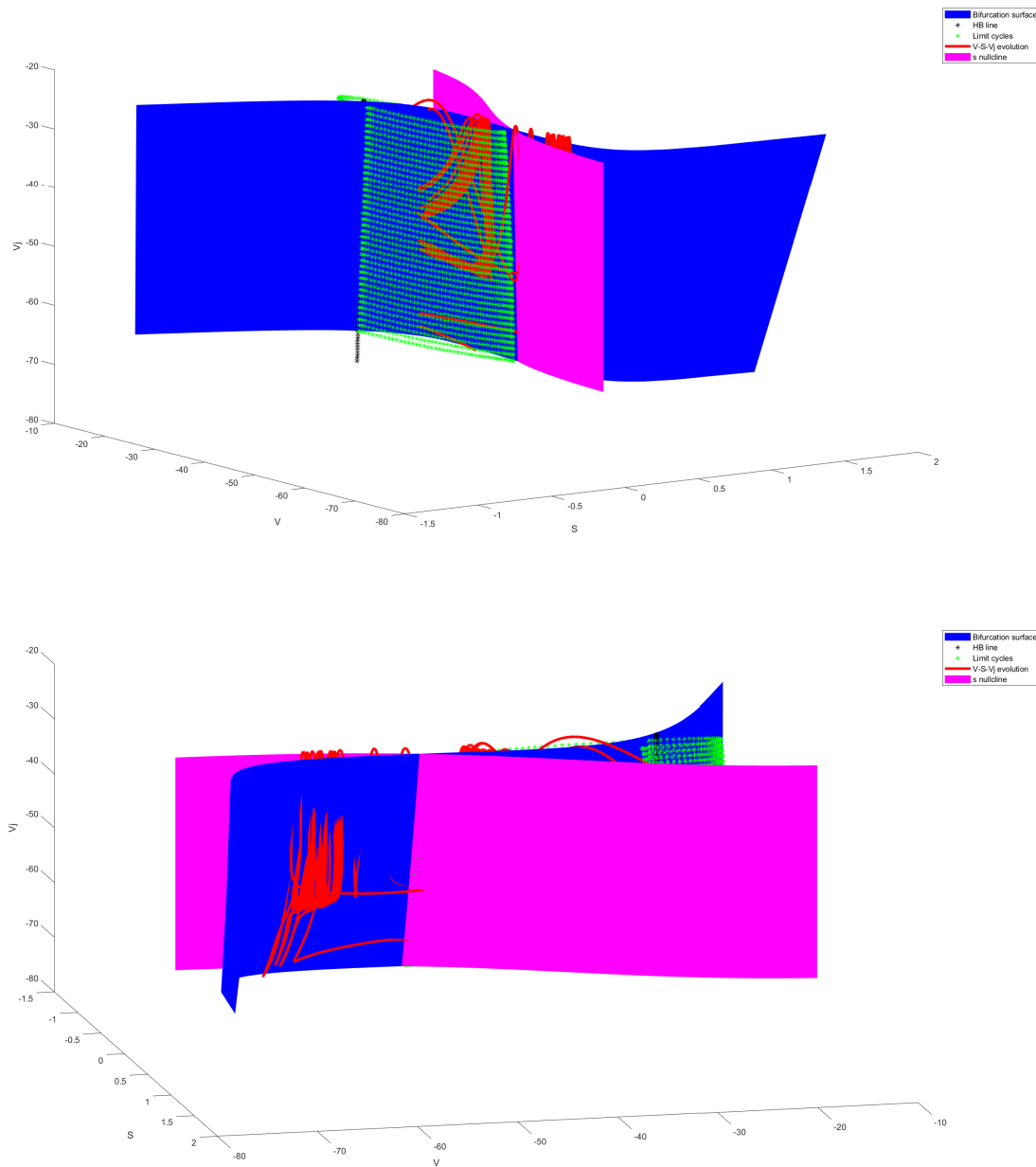


Figure 19: Blue, green and black points have the same meaning as in the figure 17. In red is presented the evolution of the cell dynamics. Two points of view are presented, so the dynamic could be observed under and over the surface.

off the stable solutions and at then fires a new big burst. This happens when the model goes through the s nullcline. To show this, in figure 19 is added the "nullcline surface" in magenta for $s=0$ and V_j in the range $-26-64$ mV, the limits of S from where the big burst are born are defined more clearly.

7 Conclusions

The primary objective of the thesis was to discover and discuss particular dynamics between two coupled cells. This was successfully obtained in the case of two heterologous cells with coupling, having one cell bursting while the other was in a resting state. The interesting patterns appeared for gc in the range 0.03-0.1, but it is worth noting that while the value increased, the quality of the pattern deteriorated. In the analysis, the best parameters to show the system behavior were 0.04 and 0.05, since for those two the pattern was very stable and clear. The secondary objective was to give a geometric explanation to the phenomenon observed, and again this was successfully obtained. Specifically, the idea of utilizing a 3D graphic facilitated the visualization and validation of the explanations offered for the 2D version. Research for interesting patterns was tried for three coupled cells in both linear and triangular configurations, but no interesting dynamics emerged. This kind of analysis with more than 2 cells is an intriguing point from which further investigations could be done, maybe going to the macroscopic cases, considering the dynamics of the single cell in the cluster.

Ringraziamenti

Vorrei inanzitutto ringraziare il professor Morten Gram Pedersen per la disponibilità, il supporto e per la pazienza che ha dimostrato durante il percorso, soprattutto quando i modelli non ne volevano sapere di funzionare.

Un grande ringraziamento ai miei genitori, per esserci sempre stati per me fin da piccolo ad oggi. Per non avermi fatto sentire i problemi della vita, per avermi insegnato la matematica, per avermi sgridato quando ce n'era bisogno, semplicemente per avermi voluto bene nonostante tutti i guai e le strane idee che fin da piccolo ho sempre avuto. Senza di voi oggi non sarei qui.

A Benny, che anche dopo dieci anni continua ad essere lì per me, nonostante le ansie e le pare rappresenta sempre la costante, la mia piccola roccia.

Il fiucia è semplicemente più bello se ci sei tu.

Agli amici del proteam, che poi si è allargato diventando la caverna! Tra discussioni, serate etc. sopportate sempre le mie uscite, davvero non lo so come facciate, a volte mi do fastidio da solo!

Ai miei 200 cugini, che nonostante le mie numerose assenze, restano la miglior famiglia che io potessi chiedere. Ma magari adesso che ho finito qua si può rimediare un po', forse, spero.

Agli amici dell'università, le giornate vissute a Padova resteranno per sempre con me, questo è anche merito vostro.

Agli amici del calcio, è stato bello tornare a vivere lo sport e lo spogliatoio. Ho reincontrato alcuni vecchi compagni e ne ho conosciuti di nuovi, siamo scarsi ma va bene così, almeno ci divertiamo fuori dal campo!

Grazie a tutti, sinceramente, da Valerio, ciao!

8 Bibliography

1. *Global report on Diabetes*, World Health Organization, 2016.
2. *Definition, Diagnosis and Classification of Diabetes Mellitus and its Complications. Part 1:Diagnosis and Classification of Diabetes Melitus (WHO/NCD/NCS/99.2)*. Geneva: World Healt Organization; 1999
3. GBD 2013 Risk Factors Collaborators. *Global, regional, and national comparative risk assessment of 79 behavioural, environmental and occupational, and metabolic risks or clusters of risks in 188 countries, 1990–2013: a systematic analysis for the Global Burden of Disease Study 2013*. Lancet. 2015;386(10010):2287–323.
4. Ley SH, Hamdy, O, Mohan V, Hu FB. *Prevention and management of type 2 diabetes: dietary components and nutritional strategies*. Lancet. 2014;383(9933):1999–2007
5. Wong E, Backholer K, Gearon E, Harding J, Freak-Poli R, Stevenson C, et al. *Diabetes and risk of physical disability in adults: a systematic review and meta-analysis*. Lancet Diabetes Endocrinology. 2013;1:(2)106–114
6. Mark A. Atkinson, Martha Campbell-Thompson, Irina Kusmartseva, Klaus H.Kaestner *Organisation of the human pancreas in health and in diabetes*, Diabetologia. 2020 October; 63(10): 1966–1973.
7. Longnecker DS, Gorelick F, Thompson ED (2018) *Anatomy, histology, and fine structure of the pancreas* In: *Beger HG, Warshaw AL, Hruban RH et al. (eds) The pancreas: an integrated textbook of basic science, medicine, and surgery*, 3rd edn John Wiley Sons Ltd, Hoboken, NJ, pp 10–23
8. Jonathan E. Campbell, Christopher B. Newgard, *Mechanisms controlling pancreatic islet cell function in insulin secretion*, Nat Rev Mol Cell Biol. 2021 February; 22(2): 142–158.
9. So Young Park, Jean-Francois Gautier, Suk Chon, *Assesment of insuline secretion and insuline resistance in Human*, Diabetes Metab J 2021;45:641-645.
10. Kevin D. Niswender, MD, *Basal Insulin: Physiology, Pharmacology, and Clinical Implications*, Postgraduate Medicine, Volume 123, Issue 4, July 2011, ISSN – 0032-5481, e-ISSN – 1941-9260
11. Daniel A. Goodenough and David L. Paul, *Gap Junctions*, Cold Spring Harb Perspect Biol 2009;1:a002576

12. Hussein Nori Rubaiy, *A Short Guide to Electrophysiology and Ion Channels*, J Pharm Pharm Sci. 2017;20:48-67.
13. William A. Catterall, Goragot Wisedchaisri, and Ning Zheng, *The Chemical Basis for Electrical Signaling*, Nat Chem Biol. 2017 April 13; 13(5): 455–463.
14. Gembal, M., P. Gilon and J.-C. Henquin. 1992. *Evidence that glucose can control insulin release independently from its action on ATP-sensitive K + channels in mouse B cells*. J. clin. Invest.89, 1288-1295.
15. Md. Shahidul Islam, *Calcium Signaling: From Basic to Bedside*, Advances in Experimental Medicine and Biology 1131
16. Xiaoyan Fang, Shukai Duan and Lidan Wang, *Memristive Hodgkin-Huxley Spiking Neuron Model for Reproducing Neuron Behaviors.*, Front. Neurosci. 15:730566.
17. Michael Hausser, *The Hodgkin-Huxley theory of the action potential*, nature, neuroscience supplement, volume 3, november 2000.
18. R. Bertram, J.E. Rubin *Multi-timescale systems and fast-slow analysis*, Mathematical Biosciences 287 (2017) 105–121
19. Arthur Sherman, *Anti-phase, asymmetric and aperiodic oscillations in excitable cells-I. COupled bursters*, Bulletin of Mathematical Biology, vol 56, No 5, pp. 811-835, 1994.
20. Gerda De Vries, Arthur Sherman, Hsiu-Rong Zhu, *Diffusively coupled bursters: Effect of cell heterogeneity*, Bulletin of Mathematical Biology (1998) 60, 1167-1200.
21. Gerda De Vries, Arthur Sherman, *Channel sharing in pancreatic β -Cells revisited: Enhancement of emergent bursting by noise*, J. theor. Biol. (2000), 207, 513-530.
22. Gerda De Vries, Arthur Sherman *From spikers to bursters via coupling: Help from heterogeneity*, Bulletin of Mathematical Biology (2001) 00, 1-21.
23. Alessandro Loppini, Morten Gram Pedersen *Gap-Junction coupling can prolong beta-cell burst period by an order of magnitude via phantom burting*, Chaos 28, 063111 (2018).

